PHYSICAL REVIEW B VOLUME 27, NUMBER 3 1 FEBRUARY 1983

Electronic density of states in amorphous zirconium alloys

F. P. Missell,* S. Frota-Pessôa,* J. Wood, J. Tyler, and J. E. Keem
Energy Conversion Devices, Inc., 1675 W. Maple Rd., Troy, Michigan 48084

(Received 6 August 1982)

We have produced amorphous Zr-Rh, Zr-Ru, and Zr-Re films by means of rf diode cosputtering techniques. Measurements were made of the superconducting transition temperature T_c, the normal resistivity ρ, and upper critical field H_{c2}. From ρ and $(dH_{c2}/dT)_{T_c}$ we determined the dressed density of states at the Fermi level $N^* = N(1+\lambda)$, where λ is the electron-phonon coupling constant and N is the bare density of states. For Zr-Rh and Zr-Re, N^* exhibited an approximately linear decrease as the Zr fraction decreased. For Zr-Ru alloys the behavior was more complex. Estimating N for Zr-Rh alloys, we find it to be approximately the same in magnitude and composition dependence as the N for Zr-Cu alloys. We calculate the magnitude and composition dependence of N for Zr-Rh and Zr-Cu alloys with the use of a simple model and obtain good agreement with the experimental results.

I. INTRODUCTION

A notable fact about amorphous superconducting transition-metal alloys is that the composition dependence of the superconducting transition temperature T_c is very different from that of their crystalline counterparts. Whereas for crystalline materials T_c shows several distinct peaks at certain values of the electron per atom (e/a) ratio (Matthias's rule), Collver and Hammond[1] showed that T_c for amorphous alloys exhibits a single broad peak centered between the two main crystalline peaks. McMillan[2] has related variations in T_c for crystalline transition-metal alloys to structure in the d-band density of states. Similarly, the effect of disorder on the density of states was considered by Crow *et al.*[3] in regard to the changes that occur in T_c of transition-metal superconductors when they are made very disordered by deposition onto cryogenic substrates. The importance of the density of states in determining T_c for amorphous transition-metal alloys has been repeatedly stressed by several authors.[4–6] Previously, Varma and Dynes[7] had highlighted the importance of the density of states in determining the properties of transition-metal superconductors.

In spite of this, however, a recent work[8] has shown that there may be exceptions to the abovementioned behavior. It was shown that amorphous alloys of $(\mathrm{Mo}_{0.6}\mathrm{Ru}_{0.4})_{1-x}\mathrm{Si}_x$ and $(\mathrm{Mo}_{1-y}T_y)_{1-x}\mathrm{Si}_x$, where T is a $4d$ or $5d$ transition metal, may have an anomalous behavior. For these materials increasing values of the electron-phonon dressed density of states N^* are associated with decreasing values of T_c. This may indicate the importance of hybridization effects of the kind usually ignored[7] by many authors. Thus this exception to the generally expected behavior motivated an examination of N^* in other amorphous superconducting alloys. There has been, furthermore, a suggestion[9] that $\mathrm{Zr}_{70}\mathrm{Ru}_{30}$ might have a T_c considerably higher than the metallic glasses $\mathrm{Zr}_{70}\mathrm{Rh}_{30}$ and $\mathrm{Zr}_{70}\mathrm{Pd}_{30}$. Therefore, we decided to fabricate alloys with compositions $\mathrm{Zr}_{1-x}\mathrm{Rh}_x$, $\mathrm{Zr}_{1-x}\mathrm{Ru}_x$, and $\mathrm{Zr}_{1-x}\mathrm{Re}_x$ and to study their superconducting properties.

In the present work we report on alloys produced by rf diode cosputtering techniques on room-temperature substrates. Previously, $\mathrm{Zr}_{75}\mathrm{Rh}_{25}$ had been fabricated by rapid quenching in a piston-and-anvil apparatus[10] and by melt spinning.[11,12] Our amorphous alloys, with compositions between $\mathrm{Zr}_{80}\mathrm{Rh}_{20}$ and $\mathrm{Zr}_{57}\mathrm{Rh}_{43}$, had slightly lower values for T_c than the $T_c = 4.3$ K reported for $\mathrm{Zr}_{75}\mathrm{Rh}_{25}$.[10–12] The values of T_c for our amorphous Zr-Ru alloys were only slightly higher than those for Zr-Rh alloys, while results for Zr-Re alloys were lower. The normal-state resistivity ρ and the temperature derivative of the upper critical field $(dH_{c2}/dT)_{T_c}$ were used to determine the dressed density of states N^* for these alloys. Both Zr-Rh and Zr-Re alloys show a linearly decreasing N^* with decreasing percentage of Zr. For Zr-Rh alloys our values of N^* are comparable to values of N^* for Zr-Cu alloys, obtained for the same range of compositions.[13] Estimating λ, the electron-phonon coupling constant for these alloys, we obtained the bare density of states $N = N^*/(1+\lambda)$ for the Zr-Rh alloys and, again, the results were in agreement with those for Zr-Cu alloys of Ref. 13. The magnitude and alloying behavior of N for the Zr-Cu and Zr-Rh alloys can be understood in terms of a simple model where we assume that the d band of Rh or Cu makes a negligible contribution to the density of states at the Fermi level. This is in accord with recent ultraviolet photoelectron spectroscopy (UPS) measurements.[14,15] Then the measured density of states is given as a sum of contributions from the Zr *d* band and the Zr and Cu or Rh *s* bands. We obtain good agreement with experiment. Although we are not in a position to estimate λ for the Zr-Re alloys, nor are there UPS measurements for these alloys, the resemblance of these data to those obtained for Zr-Rh and Zr-Cu alloys suggests that a similar explanation may be possible here. Recent studies of Zr-Ru alloys show that Ru *d* band is not as separated from the *d* band of Zr, and is somewhat wider than that of Rh. Our simple model allows us to understand in a qualitative manner the composition dependence of N^* for these materials.

II. SAMPLE PREPARATION AND EXPERIMENT

The alloys studied in this work were prepared by rf diode cosputtering techniques on round, 3-in. glass substrates maintained near room temperature. Base pressures of 10^{-6} Torr were obtained prior to initiating a flow of Ar at a pressure of 7 μm. The substrates were masked with the use of standard photolithographic techniques. The targets were of high-purity Zr, appropriately modified by high-purity foils of Rh, Ru, or Re. The substrate was arranged above the target in such a manner that a composition gradient was obtained along the substrate, furnishing a number of samples for resistivity measurements with different compositions. Similar techniques have been used previously for obtaining composition gradients.[16,17] In addition, larger regions of the disk were patterned to provide x-ray samples for determining the phases present in the deposited material. One large x-ray sample was available for each of the three resistivity samples and, therefore, the x-ray results are to be considered averages over three compositions. On the other hand, the composition of each individual resistivity sample was measured directly with the use of wavelength or energy-dispersive x-ray spectroscopy. Sample compositions should have an absolute accuracy of 5%, but a relative accuracy of 1–2 %.

All of the $Zr_{1-x}Rh_x$ alloys studied were amorphous, indicating that the amorphous phase extends, at least, from 20 at. % Rh to 43 at. % Rh. Togano and Tachikawa[18] studied liquid-quenched Zr-Rh alloys and found a noncrystalline phase corresponding to 18–26 at. % Rh. Their results for the position 2θ of the peak in x-ray intensity and full width at half maximum agree well with our results for the compositions that are common to both works. We see that we have extended the amorphous phase by at least 17 at. % to higher Rh concentrations through vapor-phase deposition. This result is consistent with the observation of a stable amorphous phase over a wide range of compositions in other Zr alloys, for example Zr-Cu (Ref. 13) and Zr-Ni (Ref. 19) alloys. For $Zr_{1-x}Ru_x$ alloys with $0.22 < x < 0.28$ we obtain x-ray traces consistent with an amorphous phase. Collver and Hammond[20] apparently obtained amorphous $Zr_{54}Ru_{46}$ ($T_c \sim 3.1$ K) by depositing onto a liquid-nitrogen-cooled substrate. Thus it seems possible to obtain the amorphous phase over a wide composition range in Zr-Ru also. Finally, in the case of the Zr-Re alloys, we find the amorphous phase to extend, at least, from 16 to 30 at. % Re. To our knowledge, this is the first report of an amorphous Zr-Re alloy.

The superconducting transition temperature T_c was determined resistively in all cases with the use of current densities of order 1–3 A/cm^2. T_c was taken to be the temperature corresponding to 50% of normal resistance. The temperatures were determined by a calibrated carbon glass thermometer. Magnetic fields up to 9 T were generated by a superconducting solenoid with a homogeneity of 0.1% over a 1-cm-diam. sphere. The upper critical field H_{c2} was studied as a function of temperature for the magnetic field perpendicular to the film surface. The field was swept at fixed temperature and the voltage drop across the sample was continuously monitored. H_{c2} was taken to be the field value corresponding to half the normal-state resistance. As for the resistivity, the sample geometry was well defined with the use of standard photolithographic techniques. Film thicknesses were determined with the use of a Dektak mechanical stylus. Thus the resistivities should be accurate to about ~5–10 %.

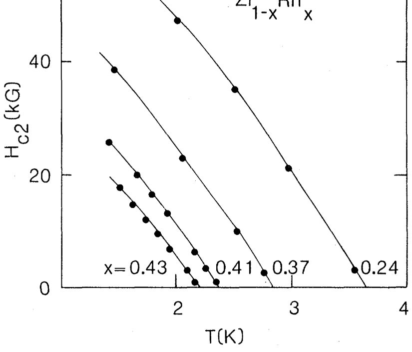

FIG. 1. Upper critical field H_{c2} as a function of temperature T for several $Zr_{1-x}Rh_x$ alloys.

TABLE I. Superconducting properties of alloys studied.

Composition	T_c (K)	$(dH_{c2}/dT)_{T_c}$ (kG/K)	ρ_{300} ($\mu\Omega$ cm)	ρ_{25} ($\mu\Omega$ cm)
$Zr_{57}Rh_{43}$	2.18 ± 0.01	26 ± 1	205	214
$Zr_{59}Rh_{41}$	2.44 ± 0.23	27	187	200
$Zr_{63}Rh_{37}$	2.86 ± 0.05	28	182	194
$Zr_{73}Rh_{27}$	3.57 ± 0.01	31	166	177
$Zr_{76}Rh_{24}$	3.67 ± 0.01	32	180	185
$Zr_{77}Rh_{23}$	3.66 ± 0.02	32	165	175
$Zr_{80}Rh_{20}$	3.72 ± 0.01	31	171	184
$Zr_{72}Ru_{28}$	3.76 ± 0.01	27		194
$Zr_{73}Ru_{27}$	3.11 ± 0.06	27	203	213
$Zr_{78}Ru_{22}$	3.73 ± 0.04	23	184	193
$Zr_{82}Ru_{18}$	3.78 ± 0.01	28	196	205
$Zr_{82}Ru_{18}$	3.33 ± 0.07	27		185
$Zr_{87}Ru_{13}$	3.57 ± 0.13	20	188	193
$Zr_{89}Ru_{11}$	3.84 ± 0.08	21		198
$Zr_{89}Ru_{11}$	3.90 ± 0.08	24	196	204
$Zr_{92}Ru_{8}$	3.79 ± 0.16	20	196	200
$Zr_{70}Re_{30}$	$2.69^{+1.06}_{-0.07}$	24	190	199
$Zr_{84}Re_{16}$	$3.32^{+0.39}_{-0.01}$	25	171	179
$Zr_{90}Re_{10}$	$4.12^{+0.20}_{-0.01}$	23	143	147

III. EXPERIMENTAL RESULTS

In Fig. 1 we show some typical curves of H_{c2} vs T for the Zr-Rh alloys. From the linear portion of the curve near T_c, we obtained $(dH_{c2}/dT)_{T_c}$ for eventual calculation of the dressed density of states. Since the lowest obtainable temperature for our system is ~ 1.5 K, we did not obtain large fractions of the H_{c2}-vs-T phase diagram for the low T_c alloys. Thus we only attempted to compare the H_{c2} curves for $x=0.23$ and 0.24 to the Ginzburg-Landau-Abrikosov-Gorkov (GLAG) theory. We note in Fig. 1 that the curves for $x=0.24$ and 0.37 are bending completely over at low T and do not show the linear behavior reported for some amorphous alloys.[21] Further analysis showed that the $x=0.23$ and 0.24 curves are in agreement with the GLAG theory. These results will be discussed elsewhere.

In Table I we give the T_c values for the Zr-Rh alloys studied here. The uncertainties in T_c represent the transition widths, corresponding to the temperature difference between 10% and 90% of the full normal resistance. For our Zr-Rh alloys most of the transitions are quite narrow. The values of T_c for our films with compositions near $Zr_{75}Rh_{25}$ are in the range 3.6–3.7 K. We note that this is somewhat lower than the value of 4.3 K reported in Ref. 10 for liquid-quenched alloys and in Refs. 11 and 12 for meltspun material. However, all of these authors reported that, upon annealing, T_c of Zr_3Rh gradually diminished by 0.2–0.3 K as the material underwent structural relaxation. Reference 10 reported that further annealing resulted in a crystalline $E9_3$ phase with $T_c \sim 2.8$–2.9 K. In the present case, however, the x-ray diffraction trace showed no sign of any Bragg peaks, indicating that the percentage of any included crystalline material was very small.

Also given in Table I are T_c values for the Zr-Ru and Zr-Re alloys. Our value for T_c of amorphous $Zr_{72}Ru_{28}$, $T_c=3.76$ K, is somewhat higher than the T_c reported by Collver and Hammond for a different composition and represents the highest T_c value reported to date for an amorphous Zr-Ru alloy. In the case of the Zr-Re alloys, we observed transitions, strongly broadened in an asymmetric fashion to the high-temperature side. Upon seeing these transitions, we suspected the presence of two phases. However, the x-ray data showed two of these samples to be amorphous and did not give indications of another phase. We are currently investigating the source of this broadening. Values of the critical-field slope at T_c, $(dH_{c2}/dT)_{T_c}$, as well as the resistivity at 25 K, ρ_{25}, and at 300 K, ρ_{300}, are also given in Table I. We note that the thermal contraction of the substrate was not taken into account in calculating ρ_{25}. Thus the use of ρ_{25} and ρ_{300} may provide unreliable values of the temperature coefficient of resistivity.

TABLE II. Electronic density of states for alloys studied.

Composition	T_c (K)	N^* (states/eV at. spin)	λ[a]	N (states/eV at. spin)[a]
$Zr_{57}Rh_{43}$	2.18	0.64	0.43	0.45
$Zr_{59}Rh_{41}$	2.44	0.72	0.48	0.49
$Zr_{63}Rh_{37}$	2.86	0.79	0.51	0.52
$Zr_{73}Rh_{27}$	3.57	1.02	0.61	0.63
$Zr_{76}Rh_{24}$	3.67	1.02	0.61	0.63
$Zr_{77}Rh_{23}$	3.66	1.09	0.64	0.66
$Zr_{80}Rh_{20}$	3.72	1.02	0.61	0.63
$Zr_{72}Ru_{28}$	3.76	0.77		
$Zr_{73}Ru_{27}$	3.11	0.71		
$Zr_{78}Ru_{22}$	3.73	0.69		
$Zr_{82}Ru_{18}$	3.78	0.81		
$Zr_{82}Ru_{18}$	3.33	0.86		
$Zr_{87}Ru_{13}$	3.57	0.63		
$Zr_{89}Ru_{11}$	3.84	0.66		
$Zr_{89}Ru_{11}$	3.90	0.73		
$Zr_{92}Ru_{8}$	3.79	0.63		
$Zr_{70}Re_{30}$	2.69	0.63		
$Zr_{84}Re_{16}$	3.32	0.79		
$Zr_{90}Re_{10}$	4.12	0.93		

[a] Estimated; see text.

IV. DISCUSSION

A. Determination of electronic density of states

According to the extended GLAG theory,[22,23] the resistivity ρ and the slope of H_{c2} near T_c are related to the electron-phonon dressed density of states for one spin direction $N^*(E_F)$ by the relation

$$\left[\frac{dH_{c2}}{dT}\right] = -\beta\frac{8kec}{\pi}\rho N^*(E_F)\ , \tag{1}$$

where β is an enhancement factor (of order 1) for strong coupled superconductors. $N^*(E_F)$ is related to the bare or band-structure density of states $N(E_F)$ by the relation

$$N^*(E_F)=(1+\lambda)N(E_F)\ ,$$

where λ is the electron-phonon—coupling parameter. Bergmann[24] used this relation to study the electronic density of states at the Fermi surface in amorphous strong coupling superconductors. Good agreement with the measured field slopes was obtained when λ was taken from tunneling measurements and $N(E_F)$ was calculated from the free-electron model. Furthermore, Shull *et al.*[25] showed for amorphous $La_{1-x}Ga_x$ foils that $N^*(E_F)$, obtained from specific-heat measurements, was in excellent agreement with values calculated from the slope of the upper critical field. More recently, von Minnigerode and Samwer[13] showed the two methods of determining $N^*(E_F)$ to be in good agreement for $Zr_{1-x}Cu_x$ alloys.

In Table II we present values of N^*, calculated with the use of Eq. (1) with $\beta=1$, for the materials studied in this work. We have presented our results in terms of the more familiar unit state/eV atom spin. To do this we must have the density of the alloy under consideration. Densities were calculated by taking a linear combination of the densities of the constituents. In the case of

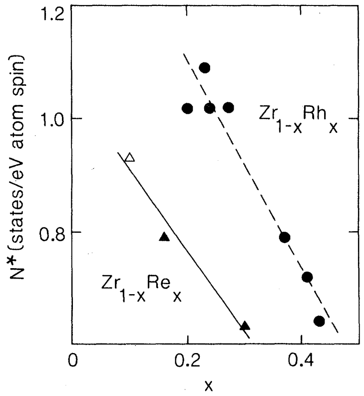

FIG. 2. Dressed density of states N^* vs x for $Zr_{1-x}Rh_x$ (●, amorphous) and $Zr_{1-x}Re_x$ (▲, amorphous; △, crystalline) alloys.

$Zr_{75}Rh_{25}$, this procedure results in a density which is $\sim 5\%$ greater than the value measured in Ref. 10. Therefore, we scaled our results by the ratio of these two values. Similarly the results for Zr-Ru alloys were scaled against the measured value of Ref. 26.

In Fig. 2 we show values of N^* as a function of x for $Zr_{1-x}Rh_x$ and $Zr_{1-x}Re_x$. Although there is some scatter in the data for $Zr_{1-x}Rh_x$, the general tendency in both cases is a decrease in N^* as the zirconium fraction decreases. We have made least-squares fits to the data points for both $Zr_{1-x}Rh_x$ and $Zr_{1-x}Re_x$ and these fits are shown in Fig. 2. We see that the slopes are approximately the same in both cases. In Fig. 3 the data for N^* of $Zr_{1-x}Ru_x$ are shown as a function of x. Here the pattern is less clear but we certainly do not see a decrease in N^* as the zirconium fraction decreases. In fact, the results of Fig. 3 seem to indicate the contrary: N^* increases with x, but in a different manner for crystalline and amorphous alloys.

As we mentioned in the Introduction, one of the purposes of this work is to investigate the correlation between N^* and T_c in these materials. Therefore, in Fig. 4 we plot T_c as a function of N^* for both $Zr_{1-x}Rh_x$ and $Zr_{1-x}Re_x$. In both cases we see that T_c increases as N^* increases. Later we will see that, for $Zr_{1-x}Rh_x$, λ is relatively small and, in fact, N follows the same trend as N^*. Thus it seems reasonable to suppose that T_c also increases with increasing N in both $Zr_{1-x}Rh_x$ and $Zr_{1-x}Re_x$. This is in agreement with previous experiments,[4–6] as well as with the calculations of Varma and Dynes[7] who suggest that N is the dominant factor in determining T_c in transition-metal superconductors. Also shown in Fig. 5 is T_c vs N^* for $Zr_{1-x}Ru_x$ alloys. Here it is difficult to discern a trend in the data, perhaps because we have only three samples which were amorphous. Nevertheless, the behavior of T_c in Fig. 5 is certainly different from that seen in Fig. 4 for $Zr_{1-x}Rh_x$ and $Zr_{1-x}Re_x$.

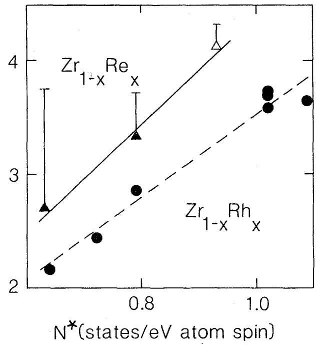

FIG. 4. Superconducting transition temperature T_c vs N^* for $Zr_{1-x}Rh_x$ (●, amorphous) and $Zr_{1-x}Re_x$ (▲, amorphous; △, crystalline) alloys. Bars for $Zr_{1-x}Re_x$ indicate transition widths.

Now in order to compare the present results with band-structure calculations, it is interesting to try to obtain N. For $Zr_{75}Rh_{25}$, Garoche and Johnson[27] found $\Theta_D = 191$ K from specific-heat measurements. Using our value $T_c = 3.67$ K and assuming $\mu^* = 0.10$, we inverted the McMillan equation to estimate $\lambda = 0.61$ for our $Zr_{75}Rh_{25}$. We note that this procedure is relatively insensitive to the exact value of Θ_D: A 5% variation in Θ_D changes λ by $\sim 1\%$.

Now in order to estimate λ for other compositions, we use a result from Varma and Dynes.[7] These authors find that λ is approximately given by

$$\lambda \sim N(E_F) W(1 \mp S) , \qquad (2)$$

where W is the width of the d band and S is related to a tight-binding overlap integral. According to Ref. 7, $W(1 \mp S)$ should be roughly constant in a class of alloys for which the dominant orbital is of the same nature at the Fermi surface. This behavior is expected for both $Zr_{1-x}Rh_x$ and $Zr_{1-x}Cu_x$,

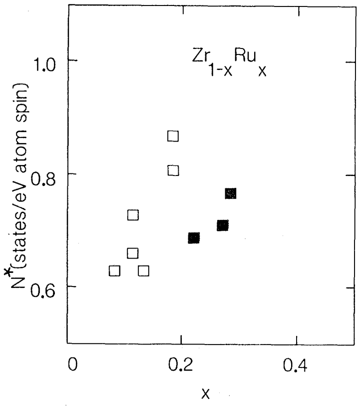

FIG. 3. Dressed density of states N^* vs x for $Zr_{1-x}Ru_x$ (■, amorphous; □, crystalline) alloys.

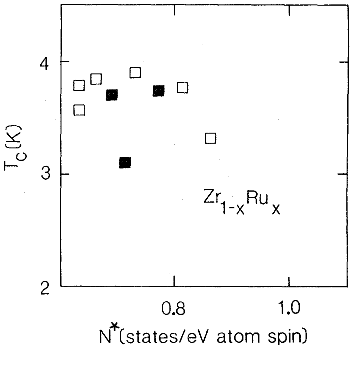

FIG. 5. T_c vs N^* for $Zr_{1-x}Ru_x$ (■ amorphous; □, crystalline) alloys.

where, as we shall see later, the Zr orbital is dominant at the Fermi level for all compositions studied. We write $\lambda \sim aN$ where a is a constant. On the other hand, we have the definition of $N^*=(1+\lambda)N$. These equations can be solved with the use of experimental values for N^* (for each x value) and the value of a from the known value of λ for $Zr_{75}Rh_{25}$. We have done this and the resulting values of λ and N are presented in Table II for the $Zr_{1-x}Rh_x$ alloys.

To evaluate this procedure for determining λ and N, we used it on the data of Ref. 13 for $Zr_{1-x}Cu_x$. In this work von Minnigerode and Samwer obtained T_c and Θ_D from specific-heat measurements and then inverted the McMillan equation to find λ and then N. We used their value of λ for $Zr_{74}Cu_{26}$ and calculated λ and N for $Zr_{50}Cu_{50}$, obtaining $\lambda=0.52$ and $N=0.46$ states/eV atom spin. von Minnigerode and Samwer obtained $\lambda=0.45$ and $N=0.475$. Although the difference in λ is slightly greater than 10%, the values of N agree to better than 5%, which seems acceptable under the circumstances.

In Fig. 6 we show N vs x for $Zr_{1-x}Rh_x$ and $Zr_{1-x}Cu_x$, the latter results obtained from Ref. 13. Within the scatter of the data the magnitudes and the concentration dependence of N are the same in Zr-Rh and Zr-Cu alloys (Fig. 6), suggesting that the Zr concentration determines N. This agrees with recent UPS measurements which show that the density of states has two peaks, the one near E_F determined by Zr and not by Rh (Ref. 15) or by Cu (Refs. 28 and 29).

B. Empirical model

To understand the behavior of the density of states we start with a simple model. In the spirit of Miedema,[30,31] we use for the total density of states a superposition of the individual density of states weighted by the concentrations. To proceed within this model we have to find the individual density of states for each component and the position of the bands relative to one another. We will limit our calculations to the cases of Cu and Rh which exhibit similar behavior and for which the bare density of states could be obtained from experiment. Nonetheless, our simple model will indicate how a completely different behavior can be obtained (as expected for Zr-Ru) alloys and illustrate the difficulties involved with this kind of calculation.

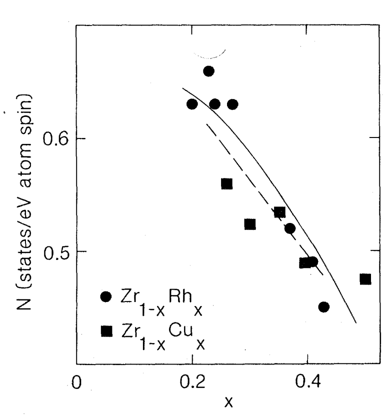

FIG. 6. Bare density of states N vs x for $Zr_{1-x}Rh_x$ and $Zr_{1-x}Cu_x$. Dashed line ($Zr_{1-x}Cu_x$) and solid line ($Zr_{1-x}Rh_x$) were calculated with model described in text.

For the individual bands we will treat the d and s states independently, ignoring s-d hybridization. For the s band we will use a free-electron model with effective mass given using the procedure described by Harrison,[32] as well as his parameters. For the d band we use the canonical band approach, based on a simplified version of the Korringa-Kohn-Rostoker method,[33] which allows us to separate the problem of calculating the density of states into two parts. The first, which depends only on structure, can be solved once and used for different materials as long as they share the structure. The second part depends on the material and essentially fixes the d-band width.

For the structural part, which fixes the shape of the band, we use the calculation of Cyrot-Lackmann[34] for amorphous Co, simulated by a dense random packing of hard spheres relaxed through a Lennard-Jones potential. To obtain the d density of states for the desired material we adjust the bandwidth with the use of the bandwidth ratio between the material we are considering and Co, while dividing the density of states by the same ratio in order to keep the number of electronic states constant. We have used, for the various elements, the widths W given by Harrison,[32] which were obtained as a best fit to crystalline calculations with the constraint of being canonically related. In Table III, W_{Zr}, W_{Cu}, and W_{Rh} are the widths of the d bands of the respective elements. In the spirit of the Slater-Koster approach, they give us an idea of the tight-binding parameters of the material. The crystalline band-structure calculations can also be used to obtain the distance E_d between the bottom of the s band and the center of the d band.[32] In Table III, E_{Zr}, E_{Cu}, and E_{Rh} are the values of E_d for the respective materials.

Having determined the band structure of each amorphous material we used the work of Gelatt *et al.*[35] to find the distance E_0 between the centers of the two bands. These are approximate values and were obtained with the use of the renormalized-atom approximation (RAA), assuming one s electron and no charge transfer. An alternative method to find E_0 could be based on the knowledge of charge

TABLE III. Parameters used to calculate densities of states for Zr-Cu and Zr-Rh alloys. All quantities are given in units of eV.

Figure	W_{Zr}	W_{Rh}	W_{Cu}	E_0	E_{Zr}	E_{Cu}	E_{Rh}
7(a)	8.37[a]		2.8[a]	4.8[b]	7.17[a]	5.9[a]	
7(b)	8.37[a]	6.89[a]		3.0[b]	7.17[a]		5.08[a]
7(c)	8.37[a]	3.0[c]		5.0[c]	7.17[a]		5.08[a]

[a] Taken from Ref. 32.
[b] Taken from Ref. 35.
[c] Taken from Ref. 37.

transfer, calculated with the use of Miedema's approach. However, as we shall see later, a more realistic model does not require charge transfer.[36] In fact, band-structure calculations by Moruzzi *et al.*[37] show that, for close-packed Zr-Rh crystalline compounds, the charge transfer is rather negligible.

Figures 7(a) and 7(b) show the density of states for Zr-Cu and Zr-Rh alloys using Harrison's parameters and the RAA values for E_0. These parameters along with those used to obtain Fig. 7(c) are listed in Table III. For Zr-Cu, alloys the Cu *d* band does not contribute at the Fermi level and N decreases with the decreasing number of Zr atoms. The density of states at the Fermi level for Zr-Cu alloys varies linearly with concentration as shown in Fig. 6, essentially reflecting the dilution of the Zr as we add Cu. It is clear from the experimental data of Fig. 6 that a similar situation should occur for Rh. Actually UPS results[15] indicate that the *d* band for Rh lies below the Zr *d* band as one might expect in this case. Therefore, Fig. 7(b), a mere superposition of bands, does not describe the Zr-Rh system well. To improve the model we will have to consider at least one feature inherent to the binary system: the effect of dilution on the bandwidth. When the bands are split and far apart in energy, the interaction between different species is less effective. As the material is diluted the average number of neighbors of the same species is smaller leading to a decreased bandwidth. The widths of both elements in the compound should be corrected as a function of composition, but the effect is far more important for the element present in low concentration. A dependence of bandwidth on the square root of concentration was obtained[38] by applying the coherent-potential theory to treat two identical bands, originating from a single level (*s* bands) and well separated in energy. These results illustrate the principle, but since we have *d* bands and an amorphous system they cannot be directly applied here.

In Fig. 7(c) we present results for our model, obtained with use of, for the Rh *d*-band width and the distance between the center of the Zr and Rh bands, parameters extracted from a band-structure calcula-

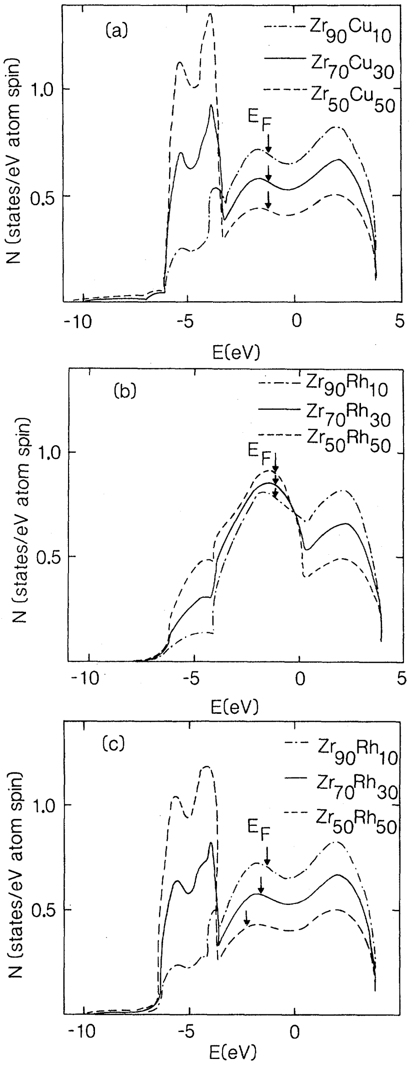

FIG. 7. (a) Bare density of states N vs energy E for $\mathrm{Zr_{90}Cu_{10}}$, $\mathrm{Zr_{70}Cu_{30}}$, and $\mathrm{Zr_{50}Cu_{50}}$, calculated with the use of the parameters of Table III. The Fermi energy E_F is marked by an arrow for each curve. (b) N vs E for $\mathrm{Zr_{90}Rh_{10}}$, $\mathrm{Zr_{70}Rh_{30}}$, and $\mathrm{Zr_{50}Rh_{50}}$, calculated with the use of the parameters of the second row of Table III. Note that $N(E_F)$ *increases* as the Zr fraction decreases. (c) N vs E for $\mathrm{Zr_{90}Rh_{10}}$, $\mathrm{Zr_{70}Rh_{30}}$, and $\mathrm{Zr_{50}Rh_{50}}$, calculated with the use of the parameters of the third row of Table III.

tion for crystalline Zr_3Rh.[38] The Zr width was not corrected, limiting the model to high Zr concentrations. As long as the *d* band of Rh is filled at the given composition (that is, as long as the Fermi level lies above the Rh *d* band), the actual width of the Rh *d* band is irrelevant for the density of states at the Fermi level. That is the reason why the model with an uncorrected *d*-band width works so well for Cu. We should note, however, that a correction of the Zr *d*-band width can be important when considering the lower Zr concentrations.

It is well worth mentioning that while the position of the Fermi level relative to the Zr band varies very little with composition, it shifts to lower energies in Zr-Rh alloys. Eventually in the limit of very small Zr concentrations, the Fermi level will lie in the Rh *d* band as it does in pure Rh. Therefore, at some concentration above 50% Rh, the density of states at the Fermi level of Zr-Rh alloys should start to increase. Moruzzi *et al.* have performed calculations for close-packed crystalline $ZrRh_3$. For this composition the density of states at the Fermi level is clearly dominated by Rh. In the copper alloy we expect it to continue to decrease since the Fermi level of Cu lies in the *s* band. We also note that due to the shift in the position of the Fermi level relative to the Zr band the variation of N in the Zr-Rh alloys deviates from a straight line. The results from Fig. 7(c) are indicated by a solid line in Fig. 6. Because the band does not have sharp features, these deviations are not significant, and due to the crudeness of the model they can be less important than effects neglected here.

Now we would like to mention a more subtle aspect of the problem that has been neglected until now. In an interacting Zr-Rh system, we expect to have some probability of finding electrons at the Zr site with energies in the range of the Rh band. By the same token, some of the Rh states are spread upwards in energy toward the Zr band. Thus it is clear that some of the states of the Rh band are actually localized on the Zr sites, explaining why a filled Rh does not necessarily imply charge transfer.

Finally, we would like to mention that calculations for crystalline Zr-Ru alloys suggest that for these materials one should have an overlap of the *d* bands leading to a more sizable contribution from Ru at the Fermi level. This case will be similar to the one illustrated in Fig. 7(b) and we do not expect for Zr-Ru alloys a pronounced decrease of N with the Zr fraction, as seen in Zr-Cu and Zr-Rh alloys.

V. CONCLUSIONS

The good agreement we have obtained for the Zr-Cu and Zr-Rh alloys suggests that other materials with split *d* bands should show a similar behavior. For high Zr concentrations UPS measurements on Zr-Pd (Ref. 14) and Zr-Ni (Ref. 29) alloys show to some degree a split *d* band and our model may provide a good account of the situation in these materials. Work is currently underway on these alloys. We have shown that, for high Zr concentrations, where distortions of the Zr band may be neglected, the behavior of the density of states in some amorphous, split-band materials can be understood in terms of a dilution effect. However, the difficulties encountered when applying the model to Zr-Rh alloys illustrate the need for more accurate methods. This is especially important if we want to have a good description for lower Zr concentrations or understand the behavior of N as a function of concentration for the case of overlapping bands. The recursion method[39] has been used to study the Zr-Cu system.[36] Efforts are under way to apply the method to study the concentration dependence of N for binary systems with overlapping bands.

ACKNOWLEDGMENTS

We wish to thank M. Tenhover for many useful discussions and V. L. Moruzzi for communicating his results prior to publication. This research benefited from the overall support of energy conversion at Energy Conversion Devices, Inc., by the Atlantic Richfield Company.

---

[*] Present address: Instituto de Física, Universidade de São Paulo, C.P. 20516, São Paulo, S.P., Brazil.

[1] M. M. Collver and R. H. Hammond, Phys. Rev. Lett. 30, 92 (1973).

[2] W. L. McMillan, Phys. Rev. 167, 331 (1968).

[3] J. E. Crow, M. Strongin, R. S. Thompson, and O. F. Kammerer, Phys. Lett. 30, 161 (1969).

[4] W. L. Johnson, J. Appl. Phys. 50, 1557 (1979).

[5] W. L. Johnson, in *Glassy Metals I*, Vol. 46 of *Topics in Applied Physics*, edited by H.-J. Güntherodt and H. Beck (Springer, New York, 1981).

[6] C. C. Tsuei, in *Superconducting Materials Science*, edited by S. Foner and B. B. Schwartz (Plenum, New York, 1981), p. 735.

[7] C. M. Varma and R. C. Dynes, in *Superconductivity in d- and f-band Metals*, edited by D. H. Douglass (Plenum, New York, 1976).

[8] J. Flasck, J. Wood, A. S. Edelstein, J. E. Keem, and F. P. Missell, Solid State Commun. 44, 649 (1982).

[9] M. Tenhover and W. L. Johnson, Physica (Utrecht) 108B-C, 1221 (1981).

[10] A. J. Drehman and W. L. Johnson, Phys. Status Solidi

A 52, 499 (1979).

[11] R. E. Elmquist and S. J. Poon, Solid State Commun. 41, 221 (1982).

[12] S. J. Poon, P. L. Dunn, R.E. Elmquist, and L. M. Smith, Solid State Commun. 42, 267 (1982).

[13] G. von Minnigerode and K. Samwer, Physica (Utrecht) 108B-C, 1217 (1981).

[14] P. Oelhafen, E. Hauser, H. J. Güntherodt, and K. H. Bennemann, Phys. Rev. Lett. 43, 1134 (1979).

[15] P. Oelhafen, V. L. Moruzzi, A. R. Williams, R. Lapka, and H. J. Güntherodt, Bull. Am. Phys. Soc. 27, 349 (1982).

[16] J. J. Hanak, J. Vac. Sci. Technol. 8, 172 (1971).

[17] A. K. Ghosh and D. H. Douglass, Phys. Rev. Lett. 37, 32 (1976).

[18] K. Togano and K. Tachikawa, J. Appl. Phys. 46, 3609 (1975).

[19] E. Babić, R. Ristić, M. Miljak, M. G. Scott, and G. Gregan, Solid State Commun. 39, 139 (1981).

[20] M. M. Collver and R. H. Hammond, Solid State Commun. 22, 55 (1977).

[21] M. Tenhover, W. L. Johnson, and C. C. Tsuei, Solid State Commun. 38, 53 (1981).

[22] G. Eilenberger and V. Ambegaokar, Phys. Rev. 158, 332 (1967).

[23] D. Rainer, G. Bergmann, and U. Eckhardt, Phys. Rev. B 8, 5324 (1973).

[24] G. Bergmann, Phys. Rev. B 7, 4850 (1973).

[25] W. H. Shull, D. G. Naugle, S. J. Poon, and W. L. Johnson, Phys. Rev. B 18, 3263 (1978).

[26] E. Raub and E. Röschel, Z. Metallk. 54, 455 (1963).

[27] P. Garoche and W. L. Johnson, Solid State Commun. 39, 403 (1981).

[28] A. Amamou and G. Krill, Solid State Commun. 28, 957 (1978).

[29] P. Oelhafen, E. Hauser, and H. J. Güntherodt, Solid State Commun. 35, 1017 (1980).

[30] A. R. Miedema, J. Phys. F 3, 1803 (1973).

[31] A. R. Miedema, J. Phys. F 4, 120 (1974).

[32] W. A. Harrison, *Electronic Structure and the Properties of Solids* (Freeman, San Francisco, 1980), Chap. 20.

[33] O. K. Andersen and O. Jepsen, Physica (Utrecht) 91B, 317 (1977).

[34] S. N. Khanna and F. Cyrot-Lackmann, Phys. Rev. B 21, 1412 (1980).

[35] C. D. Gelatt, Jr., H. Ehrenreich, and R. E. Watson, Phys. Rev. B 15, 1613 (1977).

[36] S. Frota-Pessôa (unpublished).

[37] V. L. Moruzzi, C. D. Gelatt, Jr., and A. R. Williams, Calculated Electronic Properties of Ordered Alloys (in press).

[38] B. Velický, S. Kirkpatrick, and H. Ehrenreich, Phys. Rev. 175, 747 (1968).

[39] R. Haydock, in *Solid State Physics*, edited by H. Ehrenreich, F. Seitz, and D. Turnbull (Academic, New York, 1980), Vol. 35, p. 216.